Field-Tested Method for Detecting Broken Conductors in Power Lines With Multiple Taps

Joe Livingston and Dustin Neubauer
Great River Energy

Kanchanrao Dase, Josh LaBlanc, and Aravindkumar Rajakumar
Schweitzer Engineering Laboratories, Inc.

Presented at the
62nd Annual Midwest Power Systems Conference
Saint Paul, Minnesota
November 10–12, 2026

Revised edition released October 2026

Originally presented at the
53rd Annual Western Protective Relay Conference, October 2026

Field-Tested Method for Detecting Broken Conductors in Power Lines With Multiple Taps

Joe Livingston and Dustin Neubauer, *Great River Energy*
Kanchanrao Dase, Josh LaBlanc, and Aravindkumar Rajakumar, *Schweitzer Engineering Laboratories, Inc.*

***Abstract*—Broken-conductor detection (BCD) has become increasingly important because of wildfire mitigation and public safety concerns. Most existing detection methods are developed for two- or three-terminal transmission lines and may not operate dependably on tapped or multiterminal line configurations. A novel multi-ended protection algorithm is proposed to detect a broken conductor condition occurring on any segment of a tapped line, including sections located between or on the taps. The method is based on the observation that, immediately following a broken conductor event that has not transitioned into a shunt fault, the positive-sequence voltage and load current at the taps remain largely unchanged, while the current redistributes at the line terminals. The proposed algorithm exploits this current redistribution together with zero-sequence directional supervision to provide secure and dependable detection. The paper presents an analytical evaluation of the method and validates the performance using simulation studies, a field event, and a field test conducted on a tapped transmission line. Test results demonstrate close agreement with theoretical analysis and validate the effectiveness of the proposed scheme in detecting broken conductors while maintaining security in tapped-line applications.**

I. Introduction

Growing wildfire mitigation initiatives and enhanced public safety requirements have increased the importance of broken-conductor detection (BCD) in power systems. A broken conductor, if not identified and isolated quickly, can fall to the ground and initiate ground faults, ignite surrounding vegetation, or create hazardous conditions in the proximity of the power line. Consequently, utilities are seeking protection schemes that can rapidly and dependably identify broken conductors. Furthermore, [1] demonstrates the benefits of concurrently applying BCD and traditional shunt fault protection.

Numerous single-ended and multi-ended techniques have been proposed for detecting broken conductors on overhead transmission lines in [2], [3], [4], [5], [6], and [7]. Most existing methods assume a simple point-to-point line topology and monitor changes in electrical quantities, such as voltage discontinuities, current unbalance, or sequence-component behavior. As a result, a broken conductor event occurring between tap locations or on the tap circuit can have signatures that traditional algorithms were not designed or validated to reliably detect. The dashed lines in Fig. 1 indicate portions of the line sections on a three-terminal line with load taps where traditional BCD schemes face dependability challenges.

This paper presents a dependability assessment of the existing BCD methods when applied to multiterminal and tapped power lines. The analysis highlights the need for protection schemes that remain dependable across real-world transmission line configurations.

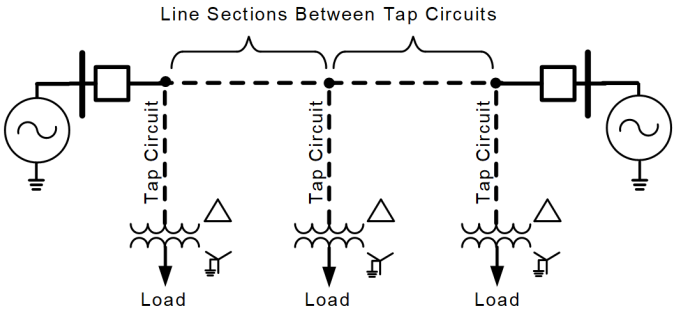


Fig. 1. Example of a tapped transmission line showing sections where traditional BCD schemes lack dependability (dashed lines).

To address the BCD dependability challenge, especially in tapped transmission lines, this paper proposes a novel multi-ended protection method capable of detecting broken conductors in any segment of a line, including those located between taps. Taps with delta-connected transformer primary windings on the line side are considered. The proposed method relies on the observation that, immediately following a broken conductor event and the extinction of the associated series arc, the positive-sequence line-terminal voltages remain largely unaffected. At this stage, the condition has not yet evolved into a shunt fault. Since the tapped loads experience negligible changes in positive-sequence voltage, the power drawn by the tapped loads remains essentially unchanged. Consequently, the positive-sequence current at the tapped load remains nearly constant before and after the broken conductor event, as is demonstrated later in this paper via field events. However, the broken conductor condition causes a redistribution of current among the line terminals, and this redistribution is used to trigger a potential broken conductor condition. For secure operation, the proposed method incorporates remote-terminal zero-sequence directional supervision to distinguish between internal and external broken conductor events.

The proposed method was validated through a field test conducted in collaboration with Great River Energy (GRE, hereafter referred to as the utility), as well as through the analysis of actual field events and Electromagnetic Transients Program (EMTP) simulation studies. During the field test, a conductor section between two tapped locations was intentionally opened using a vacuum interrupter switch to emulate a broken conductor condition. The measured results from the field test demonstrate excellent agreement with

theoretical analysis, and playback of the recorded event data further confirms the effectiveness of the proposed algorithm. Collectively, these studies demonstrate that the proposed method provides dependable detection and secure operation for tapped-line applications.

II. Dependability Assessment of Conventional BCD Schemes

Existing BCD approaches are typically developed for point-to-point line configurations and may not operate dependably when a broken conductor event occurs between tap locations or on the tap circuit. To quantify the practical impact of conventional BCD schemes described in [2], [3], [4], [5], and [6] on tapped transmission lines, the authors analyzed the utility transmission and subtransmission network, which extends throughout Minnesota, as shown in Fig. 2, and serves numerous rural electric cooperatives. This network contains a large population of rural subtransmission circuits where tapped-line configurations are common. Consequently, the utility power system provides an excellent case study and a meaningful basis for evaluating the practical limitations of conventional BCD methods.

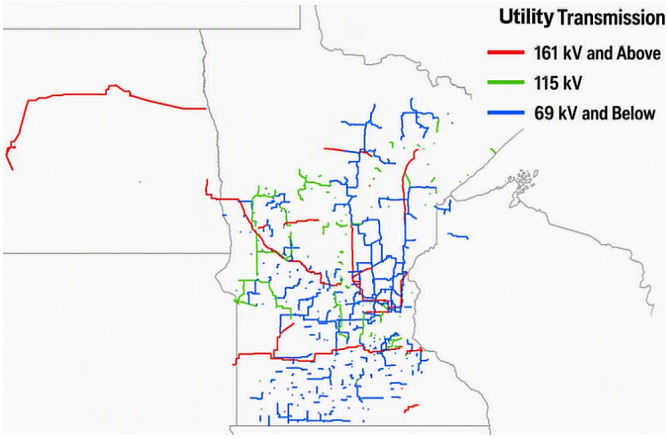


Fig. 2. Map of the utility transmission and subtransmission systems.

The utility short-circuit model was evaluated to quantify total line mileage at each voltage level and to determine the percentage of line mileage associated with tap circuits and line sections between tap locations. The outcomes of this evaluation are summarized in Table I. As expected, the prevalence of tapped-line configurations increases as system voltage decreases. This trend is apparent on the 69 kV system, where approximately 70 percent of the total line mileage is associated with tap circuits and line sections between tap locations. By comparison, approximately 11 percent of the 115 kV network has this configuration, and no such configuration exists on the 161 kV transmission system.

In summary, evaluation of the utility power system network implies that the limitations of existing BCD methods are not confined to isolated applications but can affect a substantial portion of utility infrastructure, particularly subtransmission networks. Because many of these facilities operate in rural areas with elevated wildfire risk, dependable BCD is essential for maintaining public safety and mitigating ignition hazards. These findings highlight the need for BCD schemes specifically designed to operate reliably on tapped and multiterminal transmission line configurations.

Table I
Percentage of Line Mileage Between or on Load Taps*

Voltage (kV)	Total Line Mileage (Miles)	Line Mileage Between or on Taps (Percent)
161 kV and above	6,383	0
115 kV	5,328	11
69 kV	3,026	70

* The power line mileages in Table I represent a significant portion of the interconnected transmission and subtransmission infrastructure in Minnesota.

III. Proposed BCD Algorithm for Tapped Transmission Lines

The proposed protection algorithm is designed to detect broken conductor events in tapped transmission and subtransmission lines. Specifically, the algorithm identifies whether the broken conductor event has occurred on the main power line, including line sections between the taps (shown in Fig. 1), or on an individual tap circuit.

The detection logic uses positive-sequence differential current, incremental changes in positive-sequence active power, negative-sequence differential current, and directional security checks to reliably identify the broken conductor while maintaining security for external events. The operating principles, mathematical formulations, and associated decision criteria for these quantities are presented in the following subsections. For illustrative purposes, the algorithm is described using threshold-based criteria; the corresponding threshold values, associated with positive-sequence differential current, positive- and negative-sequence current magnitudes, estimated zero-sequence voltage, and positive-sequence active power, are summarized in the Constants section of the Appendix.

Evaluation of the positive-sequence differential current requires synchronized measurements from the remote terminals. Unlike some existing BCD methods, the proposed approach is not constrained by system voltage levels. Furthermore, the use of sequence-component quantities enables the detection of single-phase and multiphase broken conductor conditions. Although the proposed algorithm is applicable to multiterminal tapped lines, the discussion focuses on a two-terminal tapped-line application for simplicity. The associated relay logic is provided in the Appendix.

A. BCD Between Tap Connections

This section considers the sequence network corresponding to a broken conductor in one of the line sections between adjacent tap locations of the system shown in Fig. 1. The resulting sequence network is illustrated in Fig. 3.

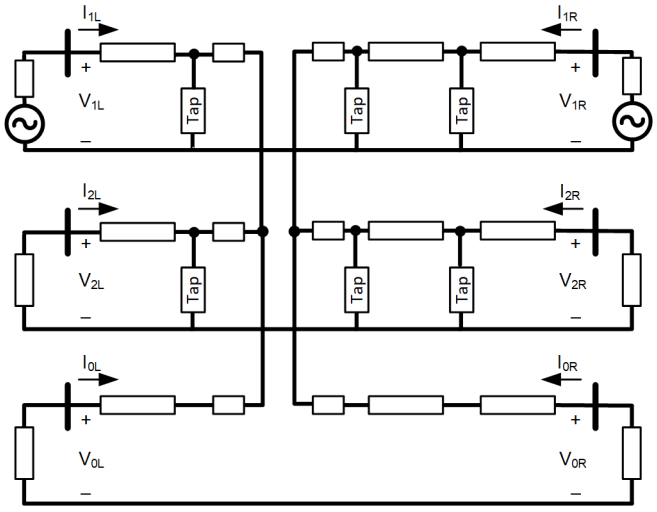


Fig. 3. Sequence network of the system in Fig. 1 for a broken conductor event between adjacent tap connections.

For the network shown in Fig. 3, $I_{1\mathrm{L}}$, $I_{2\mathrm{L}}$, and $I_{0\mathrm{L}}$ denote the positive-, negative-, and zero-sequence currents at the left terminal, respectively. Similarly, $V_{1\mathrm{L}}$, $V_{2\mathrm{L}}$, and $V_{0\mathrm{L}}$ represent the corresponding sequence voltages at the left terminal. At the right terminal, $I_{1\mathrm{R}}$, $I_{2\mathrm{R}}$, and $I_{0\mathrm{R}}$ denote the positive-, negative-, and zero-sequence currents, respectively, while $V_{1\mathrm{R}}$, $V_{2\mathrm{R}}$, and $V_{0\mathrm{R}}$ denote the corresponding sequence voltages.

The positive-sequence differential current is defined as in (1).

$$87I1 = I_{1\mathrm{L}} + I_{1\mathrm{R}} \tag{1}$$

The negative-sequence differential current is defined as in (2).

$$87I2 = I_{2\mathrm{L}} + I_{2\mathrm{R}} \tag{2}$$

The positive-sequence active power at the left terminal is defined as in (3).

$$P_{1\mathrm{L}} = |V_{1\mathrm{L}}| \bullet |I_{1\mathrm{L}}| \bullet cos(\angle V_{1\mathrm{L}} - \angle I_{1\mathrm{L}}) \tag{3}$$

The positive-sequence active power at the right terminal is defined as in (4).

$$P_{1\mathrm{R}} = |V_{1\mathrm{R}}| \bullet |I_{1\mathrm{R}}| \bullet cos(\angle V_{1\mathrm{R}} - \angle I_{1\mathrm{R}}) \tag{4}$$

Under normal operating conditions, the positive-sequence differential current of a tapped transmission or subtransmission line is non-zero and corresponds to the aggregate current supplied to the tap loads. A broken conductor occurring between a line terminal and the first tap, or between adjacent tap locations, is referred to as a main-line broken conductor event. For such an event, the positive-sequence voltage at the tap locations remains largely unchanged throughout the network unless the condition evolves into a shunt fault. As a result, the power consumed by the tap loads and the corresponding positive-sequence tap load currents experience little variation. Although the positive-sequence differential current changes little, the broken conductor condition alters the current and power-flow distribution within the protected line section. The proposed algorithm exploits these characteristics to identify a broken conductor on the main line when the following conditions are satisfied.

1) Condition 1: Minimal Change in Positive-Sequence Differential Current

The positive-sequence differential current magnitude, $|87I1|$, should remain substantially unchanged before and after the broken conductor event on the main power line. This behavior is expected because the broken conductor condition does not significantly affect the positive-sequence voltage, V_{1L} or V_{1R}. As a result, the connected taps draw nearly constant positive-sequence load currents, causing little or no observable change in the positive-sequence differential current magnitude.

2) Condition 2: Incremental Change in Positive-Sequence Active Power

For a broken conductor on the main power line, the connected tap loads continue to consume essentially the same positive-sequence active power. However, the broken conductor condition redistributes the line current and alters the power flow, P_{1L} and P_{1R}, measured at the relay terminals. To identify this condition, the algorithm verifies that the positive-sequence active power increases at one relay terminal while it decreases at the opposite terminal. These complementary power variations indicate a redistribution of power flow that is characteristic of a broken conductor on the main power line.

3) Condition 3: External Event Security Blocking

Conditions 1 and 2 may also be satisfied for broken conductor events located outside of the protected line section. Therefore, a zero-sequence directional element is included as a supervisory security measure. A zero-sequence directional element is preferred because transformers supplying tapped loads typically incorporate a delta-connected winding on the line side, which blocks the flow of zero-sequence current and effectively isolates the zero-sequence impedance of the tap loads from that of the main power line.

For a broken conductor event on the protected main line, the zero-sequence directional element may not assert in the forward direction because little or no zero-sequence voltage is developed. As a result, a permissive-based directional comparison scheme is not well suited for this application because a genuine internal broken conductor event may fail to produce a permissive signal from the remote terminal.

To improve dependability, directional supervision based on a directional comparison blocking philosophy [8] is adopted. Under this approach, operation is permitted unless a blocking signal is received from the remote terminal. Consequently, a missing blocking signal does not prevent detection of an internal broken conductor event, even when the remote directional element is unable to make a reliable directional determination because of insufficient operating voltage.

An additional security concern arises for broken conductor events located beyond the remote terminal. In such cases, the remote directional element should identify a reverse-direction condition and issue a blocking signal. However, if the event does not produce sufficient zero-sequence voltage at the remote terminal, the directional element may not operate reliably, potentially allowing the external event to be incorrectly identified as internal.

To address this condition, the algorithm supervises the directional logic using an estimate of the remote-end zero-sequence voltage. The estimate is obtained from the locally measured zero-sequence voltage and the corresponding voltage drop across the line zero-sequence impedance, as defined in (5).

$$V_{0R_{estimated}} = V_{0L} + I_{0L} \bullet Z_{0L} \quad (5)$$

The final decision logic is enabled only when the estimated remote-end zero-sequence voltage magnitude, $|V_{0R_{estimated}}|$, exceeds a minimum threshold, indicating that sufficient operating voltage is available for reliable operation of the remote directional element during external events. This additional supervision improves the security of the scheme for broken conductor events beyond the protected line section.

Accordingly, the algorithm declares a broken conductor event on the main power line when Conditions 1–3 are satisfied.

B. BCD on a Tap Circuit

This section considers a broken conductor in one of the tap circuits of the system shown in Fig. 1. The resulting sequence network is illustrated in Fig. 4.

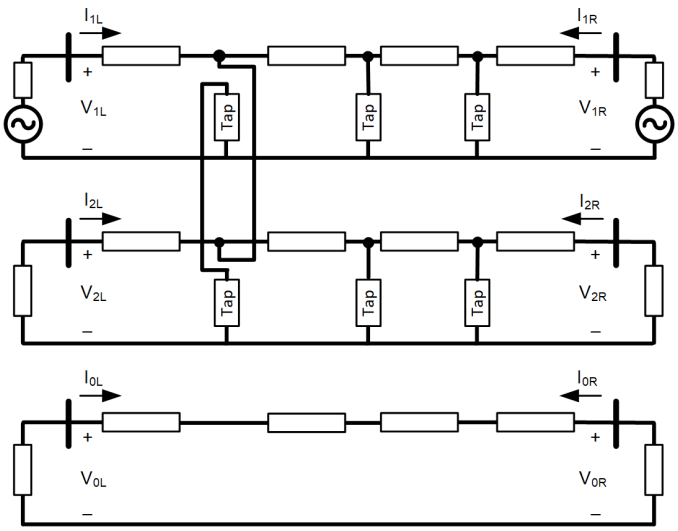


Fig. 4. Sequence network (with floating zero-sequence network) for the system in Fig. 1 for a broken conductor event in one of the tap circuits.

A broken conductor on a tap circuit directly results in a loss of load in the affected tap. Unlike a broken conductor on the main power line, in this condition the positive-sequence differential current decreases while the negative-sequence differential current increases. Based on these characteristics, the proposed algorithm declares a broken conductor on a tap or loss-of-tap-load event when the following conditions are satisfied.

1) Condition 4: Decrease in Positive-Sequence Differential Current

A broken conductor on a tap effectively disconnects the associated tap load from the system. As a result, the current contribution towards that tap decreases, causing a reduction in the measured positive-sequence differential current. Therefore, a decrease in positive-sequence differential current is used as the primary indicator of a broken conductor or an unbalanced loss-of-load condition on a tap.

2) Condition 5: Increase in Negative-Sequence Differential Current

A broken conductor condition on a tap produces an unbalanced current that gives rise to negative-sequence current. Accordingly, the algorithm uses an increase in negative-sequence differential current to confirm a broken conductor or loss-of-tap-load condition. Unlike the main-line BCD logic, this decision path does not require directional supervision because external broken conductor events do not produce the characteristic combination of a decrease in positive-sequence differential current and an increase in negative-sequence differential current.

In summary, when Conditions 4 and 5 are satisfied, the algorithm declares a broken conductor condition or an unbalanced loss-of-load event on the tap circuit.

C. Overall Detection Logic

Fig. 5 summarizes the complete detection logic. To detect a broken conductor on the main power line, the algorithm first evaluates whether the positive-sequence differential current remains substantially unchanged. If this condition is satisfied, incremental positive-sequence power flow changes are examined at the relay terminals. Following successful verification and completing directional supervisory security checks, the algorithm declares a broken conductor on the main power line.

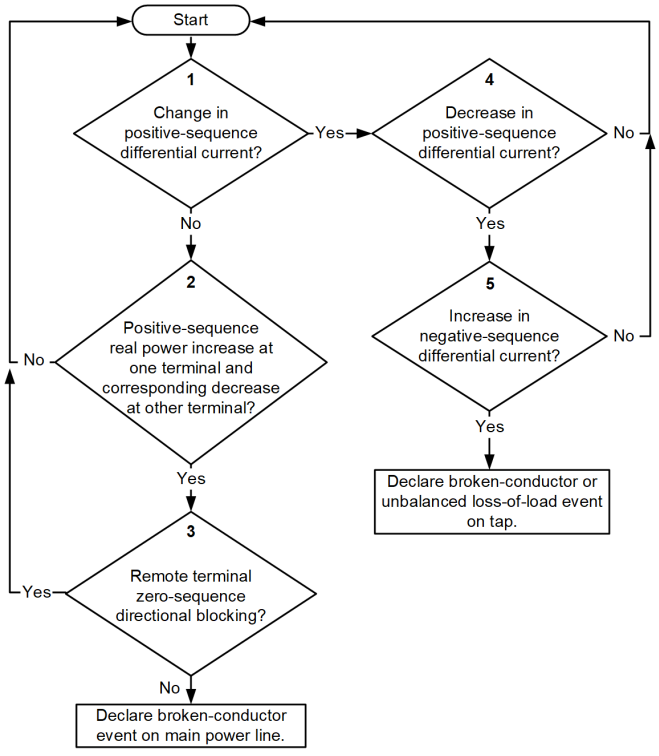


Fig. 5. Flowchart of the proposed BCD algorithm conditions for a two-terminal tapped transmission line.

To detect a potential broken conductor on a tap circuit, a decrease in positive-sequence differential current and a corresponding increase in negative-sequence differential current are monitored. When both conditions are satisfied, a

broken conductor event or an unbalanced loss-of-load event on the tap circuit is indicated.

This dual-path decision process enables reliable differentiation between broken conductor conditions occurring on the main power line and those occurring on individual tap circuits. Although the approach does not provide the exact fault location, it identifies the affected section of the system, thereby narrowing the search area to either the main line or a tap circuit and facilitating field investigation and restoration efforts.

D. Proposed Method Limitations

The proposed method relies on the redistribution of positive-sequence current following a broken conductor event on the main power line and resulting in measurable changes in the power supplied from the local and remote terminals. Consequently, a sufficient amount of interrupted load current is required for dependable operation. For example, if a line section between adjacent tap connections carries little or no load, a broken conductor event within that section may not produce a significant change in the positive-sequence current observed at the relay terminals. As a result, the associated change in positive-sequence power may be insufficient to satisfy the operating criteria, potentially preventing detection of the broken conductor event.

BCD on the main power line also depends on the availability of reliable remote terminal directional supervision. To maintain security for external broken conductor events, the algorithm employs a remote-terminal zero-sequence directional element. Reliable operation of this element requires adequate zero-sequence voltage at the remote terminal estimated from the local terminal. Because the remote terminal operating voltage is primarily established by the zero-sequence voltage drop across the protected line, the algorithm supervises the logic with a minimum zero-sequence current requirement at the local terminal. During light load conditions, or when the broken conductor event results in only a small zero-sequence current contribution, the estimated remote terminal operating voltage at the remote terminal may become insufficient for reliable directional determination. Under such conditions, the BCD algorithm is not dependable. Note that the dependency on the zero-sequence current makes the proposed method inapplicable to ungrounded or high-impedance grounded systems, as well as to parallel-line systems that share common local and remote buses. In parallel-line configurations, zero-sequence currents associated with an internal broken conductor event may circulate within the parallel-line loop, resulting in insufficient and unreliable zero-sequence voltage signals at the local and remote terminals.

In addition, a broken conductor on a tap circuit and a single-phase loss-of-load condition on the same tap have similar signatures. As a result, the proposed algorithm cannot distinguish between an unbalanced loss-of-load and a broken conductor event associated with the tap circuit. Therefore, BCD on a tap circuit is intended for alarm purposes only and is not used to initiate tripping, whereas BCD on the main power line may be used as a basis for tripping.

Conditions that produce electrical signatures similar to those of a broken conductor event may also cause operation of the proposed algorithm. Examples include an open phase resulting from a breaker pole opening, single-pole tripping, etc. To maintain security for such events, the closed-pole breaker status should be incorporated into the logic and used to supervise operation. Upon detection of an open-pole condition, a blocking signal should be transmitted to the relay at the opposite terminal to prevent undesired operation. Operation of a load switch in a line section between adjacent tap connections can also produce characteristics that resemble a broken conductor event. Accordingly, the proposed BCD algorithm should be disabled during load-switching operations on the protected power line. The security measures described in this subsection are not included in the relay logic presented in the Appendix. Utilities implementing the proposed logic are therefore encouraged to incorporate appropriate supervisory and blocking functions, including breaker-status-based security measures, to ensure secure operation.

IV. Proposed Method Validation Through Field Testing

To validate the proposed BCD method under actual operating conditions, a field test was conducted on the utility 69 kV subtransmission circuit, as shown in Fig. 6. The test was designed to emulate a broken conductor event on a tapped transmission line while maintaining customer service and overall system reliability. Event records captured during the test were compared with the analytical predictions and operating characteristics discussed in the preceding sections.

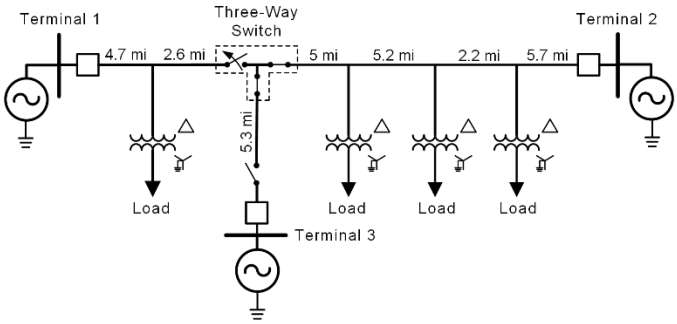


Fig. 6. Single-line diagram of the 69 kV transmission line under test.

A. Field Test Line Configuration

The subtransmission line under test normally operates as a three-terminal circuit and includes a three-way vacuum interrupter switch at the line tap location. As shown in Fig. 6, prior to the test, Terminal 3 was isolated from the test circuit. This configuration effectively converted the circuit into a 25.4-mile two-terminal subtransmission line with four load taps supplied through delta-connected transformer windings. With Terminal 3 disconnected from the main power line, only relays located at Terminal 1 and Terminal 2 were required for analysis.

The test used the three-way vacuum interrupter switch to open a single phase (A-phase) from Terminal 1 of the 69 kV line to simulate a broken conductor event rather than physically severing a conductor. Consequently, the test reproduced the steady-state electrical characteristics of a broken conductor but did not replicate the series arcing that may occur during an actual conductor failure. Because the BCD method relies on post-event current redistribution and sequence-component behavior rather than transient phenomena, the test conditions were sufficient to validate the intended operation of the algorithm.

B. Broken Conductor Emulation Using a Vacuum Interrupter

The field test used a three-way load break switch equipped with vacuum interrupters at the line tap location. Utilities apply such switches at transmission and subtransmission line taps, tie points, and sectionalizing locations where operational flexibility, line isolation, and load transfer capability are required. The compact configuration makes them particularly suitable for tapped-line applications where installation of a full switching station may not be economical.

During normal operation, a common operating mechanism controls all three phase poles simultaneously. When the switch opens, load current is interrupted with minimal external arcing while providing a visible isolation [9].

To emulate a broken conductor event, utility personnel mechanically uncoupled two poles of the motor-operated switch, allowing independent operation of the A-phase pole. This arrangement enabled the A-phase pole to open while the B- and C-phase poles remained closed, thereby emulating a single-phase broken conductor event. Fig. 7 shows the switch during the opening operation. As the switch contacts separate, a short duration arc appears at the main contact, while the load current transfers to the vacuum interrupter where current interruption occurs. The vacuum interrupter subsequently extinguishes the current, resulting in an open-phase condition without sustained external arcing.

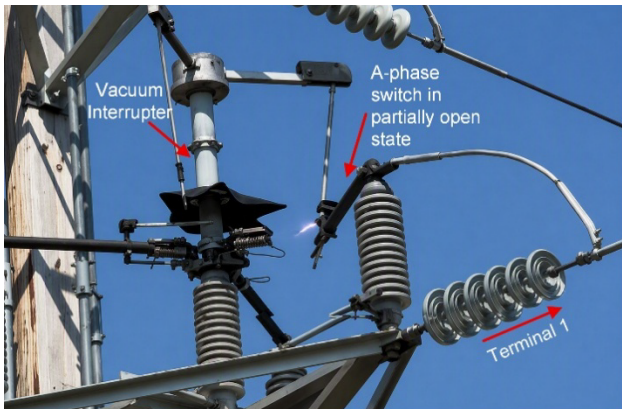


Fig. 7. Short duration arcing during operation of the A-phase switch.

Fig. 8 shows the A-phase switch in the fully open position, electrically isolating Terminal 1 from the remainder of the line through the open switch.

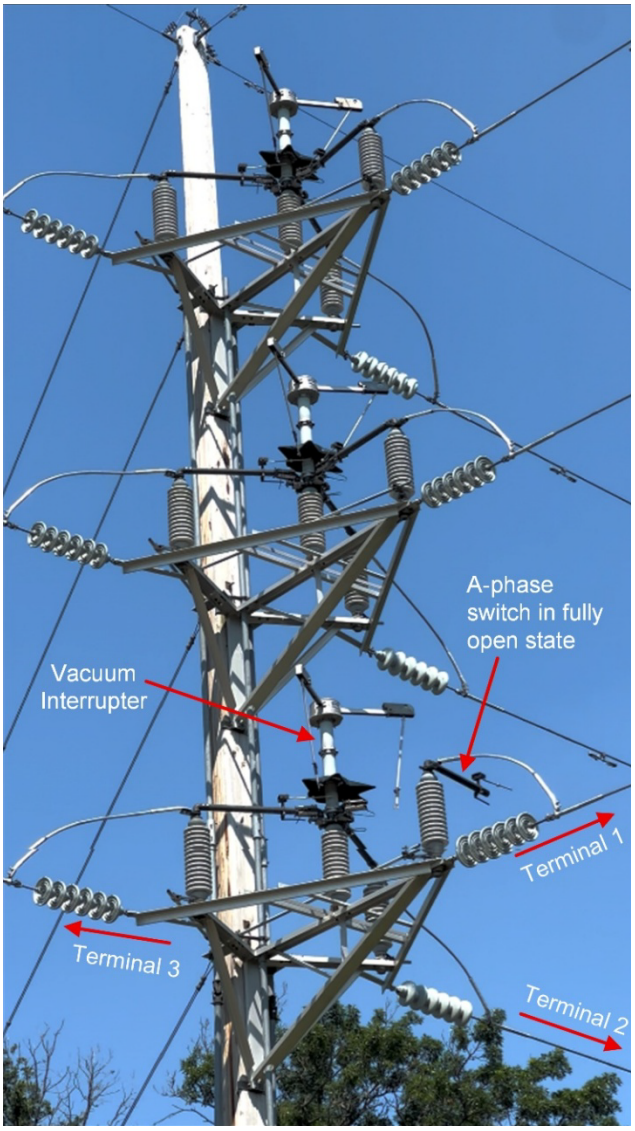


Fig. 8. A-phase switch in fully open state isolating Terminal 1 from the line.

C. Protection Settings Modifications and Event Recording

A broken conductor event excites the zero-sequence and negative-sequence networks, producing elevated zero-sequence and negative-sequence currents in the surrounding network. To prevent the operation of existing shunt fault protection during testing, the zero-sequence overcurrent elements in the line and transformer relays at Terminal 1 and Terminal 2 were evaluated and temporarily desensitized. This ensured secure operation while avoiding unnecessary customer interruptions. Negative-sequence overcurrent elements were not applied in the nearby system protection schemes. Directional element settings were reviewed to verify that the forward impedance characteristic maintained adequate separation from the origin, consistent with the recommendations in [10].

As the synchronized communications between the line terminals were unavailable, time-synchronized event reports were recorded independently at each terminal, and the proposed BCD algorithm was subsequently evaluated offline. Event triggers responding to zero- and negative-sequence currents were enabled in the relays at both terminals.

D. Staged Broken Conductor Test Execution

On the day of the test, relay technicians and engineers were stationed at both Terminal 1 and Terminal 2 substations to implement temporary settings changes and collect event data. Line crews were positioned at the tap switch location to modify the switch-operating mechanism and facilitate single-phase operation. After all personnel confirmed readiness, line crews coordinated with system operators to open the motor-operated switch, emulating the open-phase condition in A-phase at the switch, as shown in Fig. 8. Following completion of the test, the switch was reclosed, event records were verified, relay settings were restored, and the switch-operating mechanism was returned to its normal configuration.

The field test successfully produced the electrical conditions associated with a broken conductor event while maintaining continuous service to connected customers. Event records captured at both terminals exhibited the current redistribution and sequence-component behavior predicted by the analytical assessment. The following section compares the measured results with the expected operating characteristics of the proposed BCD algorithm.

V. Proposed BCD Method Performance Evaluation

The proposed BCD algorithm was evaluated from staged field test records, analysis of an actual field event, and EMTP simulation studies. The objective of this evaluation is to verify the dependability of the algorithm for broken conductor events occurring on the main power line and tap circuits, while also demonstrating security for external broken conductor events. The following case studies illustrate the operating characteristics of the proposed method and validate the detection criteria presented in Section III.

A. Staged Broken Conductor Event

During this test, the A-phase conductor on the main power line was intentionally opened through a vacuum interrupter switch as shown in Fig. 8. As discussed previously, the vacuum interrupter eliminated sustained series arcing during the switching operation. Fig. 9 shows the phase current contributions from Terminal 1 (1:IA, 1:IB, and 1:IC) and Terminal 2 (2:IA, 2:IB, and 2:IC) before and after the A-phase switch opened.

Prior to the event, both terminals supplied the tapped loads, as indicated by the positive-sequence load current measurements summarized in Table II. After the conductor opened, the current contributions from the two terminals were redistributed while the tapped loads continued to receive power. As expected, the positive-sequence differential current remained essentially unchanged despite the redistribution of terminal contributions. This behavior satisfies Condition 1 of the proposed algorithm, described in Section III.A.1.

Fig. 9 also shows the impact of the event on terminal active power contributions. Following the current redistribution, Terminal 1 increased its positive-sequence active power contribution, as indicated by 1:MW in Fig. 9, while Terminal 2 decreased its contribution, as indicated by 2:MW. Both 1:MW and 2:MW plots are expressed in megawatts and summarized in Table III. The tapped loads continued to consume approximately the same total power before and after the conductor opening. These complementary changes in terminal active power satisfy Condition 2 of the algorithm, described in Section III.A.2.

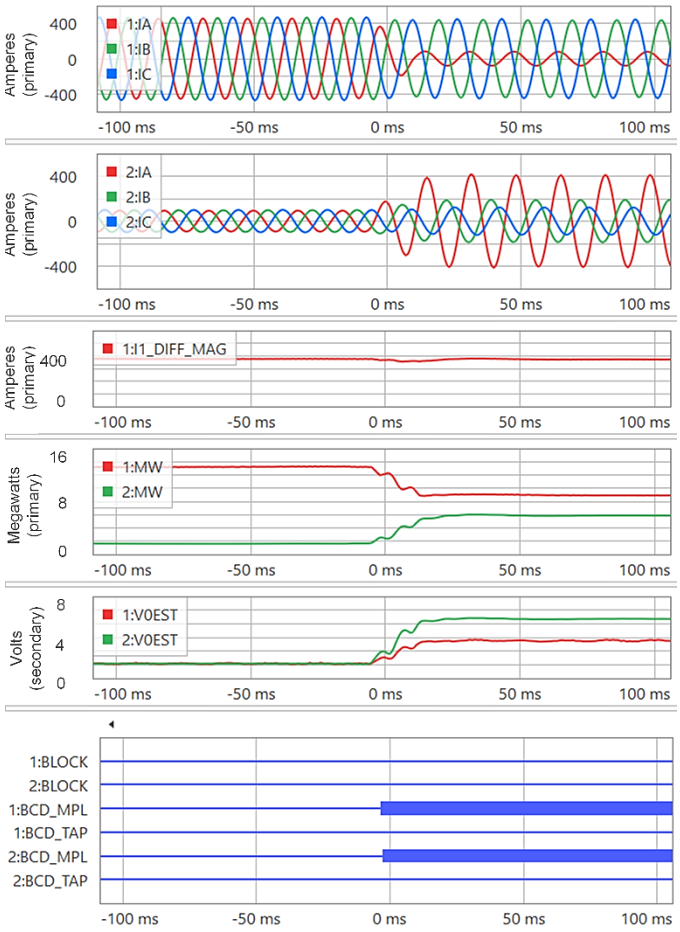


Fig. 9 Currents, megawatts, estimated remote-end zero-sequence voltage, and blocking signals at Terminals 1 and 2 for the broken conductor event between tap locations.

TABLE II
POSITIVE-SEQUENCE CURRENT (A) AT TERMINALS 1 AND 2 BEFORE AND AFTER THE BROKEN CONDUCTOR EVENT BETWEEN TAP LOCATIONS

	Terminal 1	Terminal 2	Positive-Sequence Differential Current Magnitude
Before	325∠–7°	68∠–53°	375
After	220∠–2°	159∠–22°	373

TABLE III
POSITIVE-SEQUENCE ACTIVE POWER (MW) AT TERMINALS 1 AND 2 BEFORE AND AFTER THE BROKEN CONDUCTOR EVENT BETWEEN TAP LOCATIONS

	Terminal 1 (1:MW)	Terminal 2 (2:MW)
Before	13.2	1.6
After	8.9	5.9

To verify Condition 3, the relay at each terminal estimates the remote-terminal zero-sequence voltage and verifies that sufficient operating voltage exists to reliably identify a reverse-direction disturbance. Fig. 9 shows the estimated remote-

terminal zero-sequence voltages, denoted by 1:V0EST and 2:V0EST, at Terminals 1 and 2, respectively. Both quantities are expressed in secondary volts and remain sufficiently high to support reliable reverse-direction detection and blocking, if required.

Because the broken conductor event occurred within the protected line section, neither relay identified a reverse-direction disturbance and, consequently, neither relay asserted a blocking signal, indicated by 1:BLOCK and 2:BLOCK in Fig. 9. After satisfying Conditions 1 through 3, the algorithm correctly identified the event as a broken conductor on the main power line. The corresponding detection outputs, 1:BCD_MPL and 2:BCD_MPL, asserted at Terminal 1 and Terminal 2, respectively, as shown in Fig. 9.

In Fig. 9, the deasserted 1:BCD_TAP and 2:BCD_TAP bits correctly indicate that no broken conductor event was identified on any tap circuit.

B. Broken Conductor Field Event Between the Relay Terminal and the First Tap

This field event involved a B-phase broken conductor located between the relay terminal and the first tap, as shown in Fig. 10. Unlike the staged field test discussed previously, in which the broken conductor condition occurred between tap locations, this event occurred between the relay terminal and the first tap. Because the broken conductor event occurred within the line section between the relay terminal and the first tap, the Kirchhoff's current-law-based method successfully detected the event [3]. Generally, the charging current method can also detect the event when the shunt capacitance current between the relay terminal and the broken conductor location is sufficient [2].

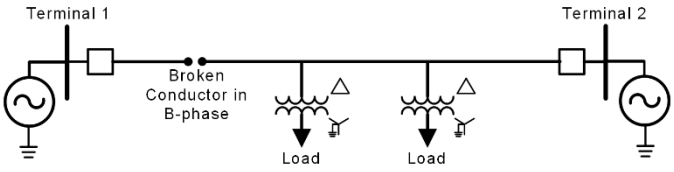


Fig. 10. Single-line diagram of a 60 kV transmission line with a broken conductor in B-phase.

As shown in Fig. 11, the event produced sustained series arcing during conductor separation. The multicycle attenuation in B-phase current waveform indicates the presence of series arcing prior to arc extinction. Consequently, series-arcing-based BCD algorithms [7] can successfully detect this event. The proposed algorithm also correctly identified the event. Fig. 11 shows that the positive-sequence differential current remained essentially unchanged throughout the broken conductor event despite the presence of sustained series arcing. This behavior satisfies Condition 1 of the proposed algorithm.

Table IV shows positive-sequence current before and after the broken conductor event at Terminal 1 and Terminal 2.

Although the positive-sequence differential current remained nearly constant, the broken conductor event redistributed the current contributions from Terminal 1 and Terminal 2. This redistribution altered the active power contributions supplied from each terminal to the tapped loads. As shown in Fig. 11 and summarized in Table V, Terminal 1 exhibited a slight increase in active power contribution after arc extinction, while Terminal 2 exhibited a corresponding decrease. These complementary changes in terminal active power satisfy Condition 2 of the algorithm.

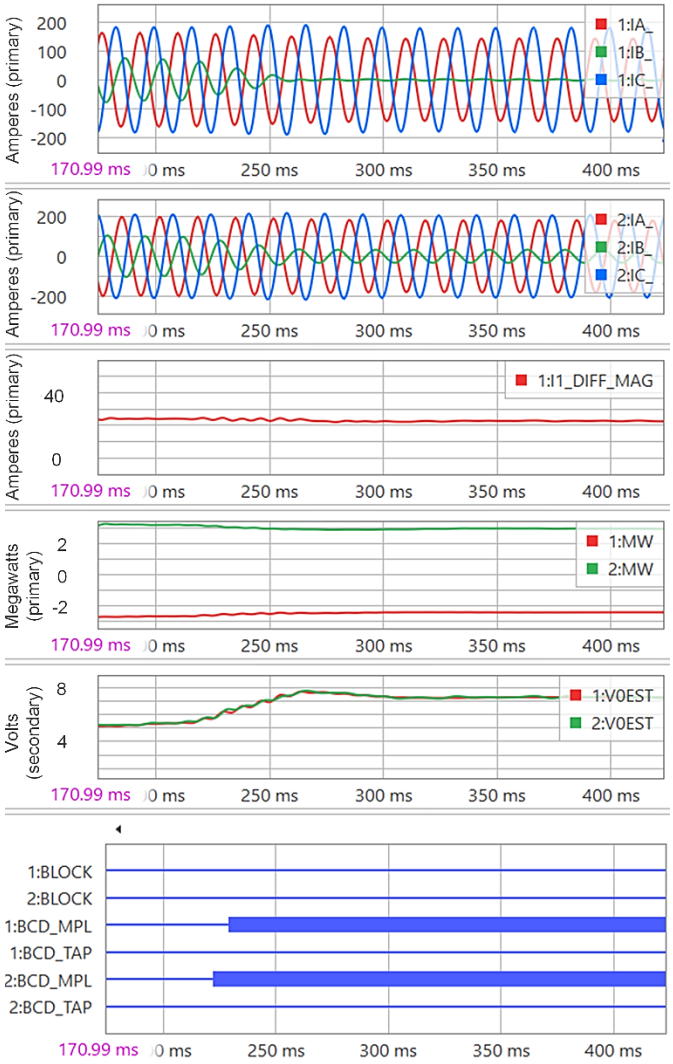


Fig. 11. Currents, megawatts, estimated remote-end zero-sequence voltage and blocking signal for the broken conductor event between the relay terminal and the first tap.

TABLE IV
POSITIVE-SEQUENCE CURRENT (A) AT TERMINALS 1 AND 2 BEFORE AND AFTER THE BROKEN CONDUCTOR EVENT BETWEEN THE RELAY TERMINAL AND THE FIRST TAP

	Terminal 1	**Terminal 2**	**Positive-Sequence Differential Current Magnitude**
Before	100∠–138°	120∠36°	23
After	79∠–149°	101∠–28°	23

TABLE V
POSITIVE-SEQUENCE ACTIVE POWER (MW) AT TERMINALS 1 AND 2 BEFORE AND AFTER THE BROKEN CONDUCTOR EVENT BETWEEN THE RELAY TERMINAL AND THE FIRST TAP

	Terminal 1 (1:MW)	**Terminal 2 (2:MW)**
Before	–2.74	3.28
After	–2.45	2.99

To verify Condition 3, each relay estimated the zero-sequence voltage at the opposite terminal to ensure sufficient operating quantity for dependable directional supervision. Fig. 11 shows that the estimated remote-terminal zero-sequence voltage remained adequate for reliable reverse-direction detection. However, because the disturbance occurred within the protected line section, neither relay asserted reverse direction and neither terminal issued a blocking signal. Thus, all three conditions of the proposed algorithm were satisfied, and the event was correctly classified as a broken conductor on the main power line.

This field event demonstrates that the proposed algorithm can reliably detect broken conductors not only between tap locations but also in the line section between a relay terminal and the first tap. Consequently, the algorithm provides dependable coverage for broken conductor events occurring anywhere on the main power line.

C. *EMTP Simulation Case 1: Security Assessment for External Broken Conductor Event*

The previous two field events demonstrated the dependability of the proposed algorithm for detecting broken conductors on the main power line. This EMTP-simulated case evaluates the security of the algorithm for an external broken conductor event. As shown in Fig. 12, a broken conductor condition was simulated outside the protected line section.

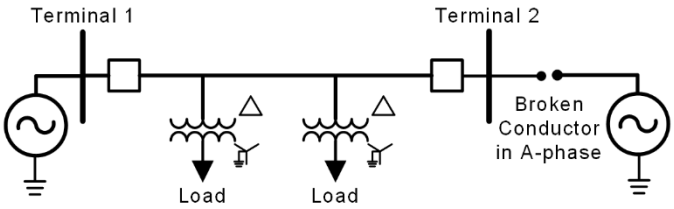


Fig. 12. Single-line diagram of a 115 kV transmission line with an out-of-zone broken conductor in A-phase.

Table VI shows that the positive-sequence differential current magnitude remained essentially unchanged before and after the broken conductor event, satisfying Condition 1 of the proposed algorithm. In addition, the broken conductor redistributed the current contributions from the line terminals.

TABLE VI
POSITIVE-SEQUENCE CURRENT (A) AT TERMINALS 1 AND 2 BEFORE AND AFTER THE BROKEN CONDUCTOR EVENT OUTSIDE THE PROTECTED LINE SECTION

	Terminal 1	**Terminal 2**	**Positive-Sequence Differential Current Magnitude**
Before	159∠−28°	73∠−38°	232
After	216∠−32°	20∠20°	229

As summarized in Table VI and shown in Fig. 13, Terminal 1 increased its active power contribution while Terminal 2 exhibited a corresponding decrease. The tapped loads continued to receive approximately the same total power before and after the event. These complementary changes in terminal active power satisfy Condition 2 of the algorithm.

TABLE VII
POSITIVE-SEQUENCE ACTIVE POWER (MW) AT TERMINALS 1 AND 2 BEFORE AND AFTER THE BROKEN CONDUCTOR EVENT OUTSIDE THE PROTECTED LINE SECTION

	Terminal 1 (1:MW)	**Terminal 2 (2:MW)**
Before	9.6	3.6
After	12.5	1.1

To verify Condition 3, each relay estimated the zero-sequence voltage at the opposite terminal to ensure sufficient operating quantity for reliable directional supervision. The estimated remote-terminal zero-sequence voltage remained adequate for dependable reverse-direction detection. Because the broken conductor event occurred beyond Terminal 2, the relay at Terminal 2 identified the disturbance in the reverse direction and asserted the blocking signal, as shown in Fig. 13. Consequently, the proposed algorithm restrained and did not declare a broken conductor event either on the protected main power line or on the tap circuit.

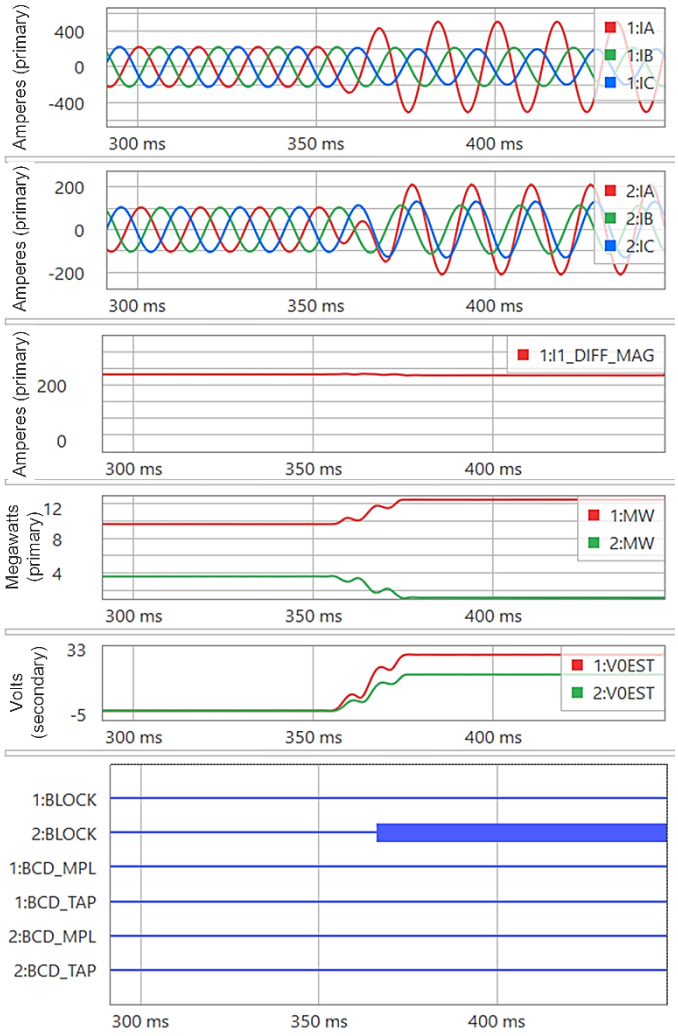


Fig. 13. Currents, megawatt (MW), estimated remote-end zero-sequence voltage, and blocking signal at Terminals 1 and 2 for the broken conductor event outside the protected line section.

The results presented in Sections V.A, B, and C demonstrate the dependability of the proposed algorithm for broken conductor events occurring within the protected line section and

enhanced security for broken conductor events outside the protected zone.

D. Simulation Case 2: Detection of a Broken Conductor on a Tap Circuit

The previous three events demonstrated dependability and security of the proposed algorithm for detecting broken conductors on the main power line. This event demonstrates the capability of the algorithm to identify a broken conductor on a tap circuit. Fig. 14 shows a simulated A-phase broken conductor on a tap circuit connected to the protected line.

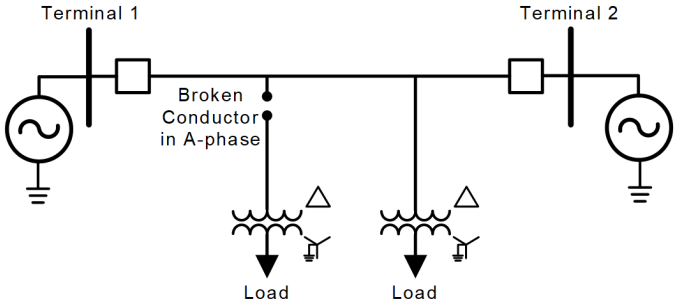


Fig. 14. Single-line diagram of a 115 kV transmission line with a broken conductor on the tap circuit in A-phase.

The A-phase tap load is lost when the broken conductor event occurs, resulting in a reduction in the positive-sequence current contribution associated with the affected tap. As shown in Table VIII and Fig. 15, the positive-sequence differential current decreases after the event. This decrease indicates either an unbalanced loss-of-load condition or an open-phase condition on the tap circuit and satisfies Condition 4 of the proposed algorithm, described in Section III.B.1.

TABLE VIII
POSITIVE-SEQUENCE CURRENT (A) AT TERMINALS 1 AND 2
BEFORE AND AFTER THE BROKEN CONDUCTOR EVENT ON A TAP CIRCUIT

	Terminal 1	**Terminal 2**	**Positive-Sequence Differential Current Magnitude**
Before	207∠−19°	86∠−91°	247
After	187∠−16°	75∠−107°	200

As shown in Fig. 15 and summarized in Table IX, the broken conductor also introduces current unbalance and generates negative-sequence current. Consequently, an incremental increase in the negative-sequence differential current provides additional confirmation of an unbalanced operating condition. The increase in negative-sequence differential current satisfies Condition 5 of the algorithm. Together, the reduction in positive-sequence differential current and the increase in negative-sequence differential current provide a reliable indication of either an unbalanced loss-of-load condition or a broken conductor on the tap circuit.

In cases where the broken conductor event produces sustained series arcing, the series-arcing-based BCD methods can also operate and provide an independent indication of a broken conductor event on the tap circuit. The combined application of the proposed algorithm and series-arcing-based detection enhances the ability to distinguish between a broken conductor condition and an unbalanced loss-of-load event on the tap circuit.

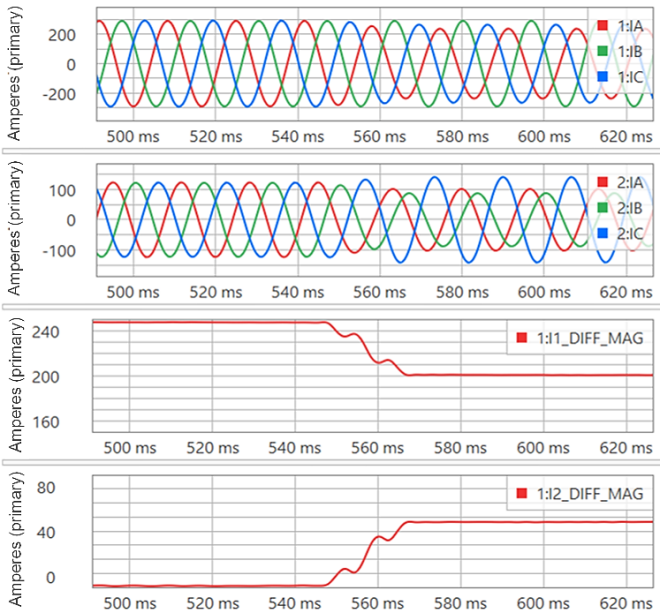


Fig. 15. Currents at Terminals 1 and 2 for the broken conductor event on a tap circuit, shown in Fig. 14.

TABLE IX
NEGATIVE-SEQUENCE CURRENT (A) AT TERMINALS 1 AND 2
BEFORE AND AFTER THE BROKEN CONDUCTOR EVENT ON A TAP CIRCUIT

	Terminal 1	**Terminal 2**	**Negative-Sequence Differential Current Magnitude**
Before	0	0	0
After	22∠133°	24∠144°	46

This event demonstrates the ability of the proposed algorithm to reliably identify broken conductor conditions on tap circuits in addition to broken conductor events occurring on the main power line.

VI. CONCLUSION

The proposed algorithm addresses a key limitation of existing BCD methods for tapped transmission and subtransmission lines. Unlike conventional approaches, which often exhibit reduced dependability for line sections located between adjacent tap connections, the proposed method provides dependable detection across these sections while also distinguishing between events occurring on the main power line and those occurring on individual tap circuits. Because the line sections between taps typically represent the largest portion of the protected corridor, especially in subtransmission networks with numerous tapped loads, the proposed approach maximizes practical detection coverage and overall dependability while maintaining security for external broken conductor conditions.

Field tests, field events, and EMTP simulation studies demonstrate that the proposed algorithm provides a dependable and secure solution for detecting broken conductor conditions on tapped transmission lines.

Since a broken conductor and a single-phase loss-of-load on a tap have similar signatures, the algorithm reports both conditions as a combination of an unbalanced loss-of-load and broken conductor event on the tap circuit. For broken conductor events accompanied by sustained series arcing, a series-arcing-based detection method can be used along with the proposed algorithm to provide a reliable indication of a broken conductor on the tap circuit.

The sensitivity of the proposed method depends on the magnitude of current interrupted by the broken conductor. Reliable detection requires sufficient current redistribution among the line terminals to produce measurable changes in the terminal power flow. Although the proposed method relies on time-synchronized current measurements, the operating principles presented in this paper could also support a single-ended implementation based on local measurements and permissive signaling.

Overall, the proposed algorithm extends dependable BCD to the sections of tapped transmission and subtransmission lines that are least effectively covered by existing methods, thereby providing a practical and secure solution for improving system protection.

VII. Appendix

This section presents instructions for the proposed algorithm implementation for a two-terminal tapped line, shown in Fig. 5, using relay logic control equations. The operating principles described in this paper are not specific to a particular relay platform and can be implemented in any protection system with access to synchronized local and remote terminal measurements and the required sequence quantities. Refer to [8] for the relay variable definitions and protection elements used in the implementation. The logic associated with 87T1P1, 87T2P1, and 87T3P1 represents the transmission of line current differential communication bits and should be implemented using available 87L transmit bits.

The relay logic presented in this appendix does not include the supervisory and blocking functions required to maintain security during breaker-pole-open conditions, single-pole tripping, or load-switching operations on the main power line. Utilities applying the proposed scheme are therefore encouraged to incorporate appropriate breaker-status-based supervision and blocking logic to ensure secure operation under these conditions, as discussed in Section III.D. Furthermore, the relay implementation presented herein uses negative-sequence current instead of the negative-sequence differential current described in Section III, with no significant impact on the performance of the scheme.

```
#### CONDITION-1 ####
PMV01:= (87I1LM*COS(87I1LA) +
87I1R1M*COS(87I1R1A)) *
(87I1LM*COS(87I1LA) +
87I1R1M*COS(87I1R1A))
PMV02:= (87I1LM*SIN(87I1LA) +
87I1R1M*SIN(87I1R1A)) *
(87I1LM*SIN(87I1LA) +
87I1R1M*SIN(87I1R1A))
PMV03:= SQRT(PMV01+PMV02) ##10-CYCLE
AVERAGED POSITIVE-SEQUENCE DIFFERENTIAL
CURRENT
PMV04:= 87I1FM*(1.000000 - AMV001)
PMV05:= 87I1FM*(1.000000 + AMV001)
PSV01:= PMV03>PMV04 AND PMV03<PMV05 AND
PMV03>AMV002 AND 87I1FM>AMV002

#### CONDITION-2 ####
PMV06:= V1FIM*LI1FIM*COS(V1FIA - LI1FIA) -
V1M*LI1M* COS(V1A -
LI1A)*1000/AMV011/AMV010
PMV07:= LI1M/AMV010
PSV02:= PMV07>AMV003 AND LI1FIM>AMV003 AND
NOT LOP
PSV03:= (PMV06>AMV004 AND 87R02P1 AND
PSV02) OR (PMV06<AMV005 AND 87R01P1 AND
PSV02) ##87R02P1 INDICATES DECREASE IN P1,
87R01P1 INDICATES INCREASE IN P1
#87T1P1:= PMV06>AMV004 AND PSV02 ##87
TRANSMIT BIT 1, INDICATES INCREASE IN
POSITIVE-SEQUENCE ACTIVE POWER MAGNITUDE
#87T2P1:= PMV06<AMV005 AND PSV02 ##87
TRANSMIT BIT 2, INDICATES DECREASE IN
POSITIVE-SEQUENCE ACTIVE POWER MAGNITUDE

#### CONDITION-3 ####
PMV08:= 3V0FIM + LIGFIM*AMV006
PSV04:= PMV08>AMV007 AND NOT 87R03P1
PMV09:= 3V0FIM*LIGFIM*COS(3V0FIA - LIGFIA
- AMV008)
#87T3P1 := PMV09 > 0 AND 3V0FIM > AMV007 #
87 TRANSMIT BIT 3, INDICATES REVERSE FAULT
#### PCT01Q INDICATES BCD BETWEEN TAPS
####
PCT01IN:= PSV01 AND PSV03 AND PSV04 AND
NOT 87T3P1
PCT01PU:= 2
PCT01DO:= 0

#### CONDITIONS-4 and 5 ####
PMV10:=(L3I2FIM*COS(L3I2FIA) - L3I2M*
COS(L3I2A)/AMV010)*(L3I2FIM*COS(L3I2FIA) -
 L3I2M* COS(L3I2A)/AMV010)
PMV11:= (L3I2FIM*SIN(L3I2FIA) - L3I2M*
SIN(L3I2A)/AMV010)*(L3I2FIM*SIN(L3I2FIA) -
 L3I2M* SIN(L3I2A)/AMV010)
PMV12:= SQRT(PMV10 + PMV11) ##INCREMENTAL
NEGATIVE-SEQUENCE CURRENT
PSV05:= PMV03>PMV05 AND PMV03>AMV002 AND
87I1FM>AMV002 AND PMV12>AMV009 AND
L3I2FIM>AMV009
#### PCT02Q INDICATES BCD OR LOSS OF
UNBALANCED LOAD IN THE TAP ####
```

```
PCT02IN := PSV05
PCT02PU := 2.000000
PCT02DO := 0.000000

#### CONSTANTS ####
AMV001:= 0.05 ##AMV001 (E.G. 0.05 PU) IS THRESHOLD MARGIN TO COMPARE PRE AND DURING OPEN PHASE I1 DIFFERENTIAL
AMV002:= 0.1 ##AMV002 (E.G. 0.1 PU) IS THE MINIMUM I1 DIFFERENTIAL CURRENT THRESHOLD
AMV003:= 0.05 * AMV012 ##AMV003 (E.G. 0.05*INOM) IS THE MINIMUM LOCAL POSITIVE-SEQUENCE CURRENT THRESHOLD
AMV004:= 0.01 * SQRT(3) * AMV014 * AMV012 / 3 #AMV004 = 0.01*SQRT(3)*VNOMY*INOM/3
AMV005:= -AMV004
AMV006:= AMV013 ##AMV006 (Z0MAG) IS THE TOTAL ZERO-SEQUENCE IMPEDANCE MAGNITUDE IN SECONDARY
AMV007:= 3 ##AMV007 (E.G. 3V) IS THE MINIMUM THREE TIMES ZERO-SEQUENCE VOLTAGE MAGNITUDE IN SECONDARY AT REMOTE END TO RELY ON ANGLE CHECK
AMV008:= 65 ##AMV008 (Z0ANG) IS THE ZERO-SEQUENCE IMPEDANCE ANGLE
AMV009:= 0.05 ##AMV009 (E.G. 0.05 A, SEC) IS THRESHOLD MARGIN FOR INCREMENTAL I2 MAGNITUDE CHECK
AMV010:= 120 ##CTR
AMV011:= 1000 ##PTR
AMV012:= 5 ##INOM
AMV013:= 14.4 ##Z0MAG
AMV014:= 115 ##VNOMY
```

VIII. Acknowledgments

The authors gratefully acknowledge the contributions of the field personnel who supported the planning and execution of the field testing. The authors thank relay technicians Scott Overbye, Corey Gilbertson, Brandon Schlangen, Dan Schirmers, and Alex Heaney, and line technicians Derek Marcoullier, Grant Hess, Brent Benjamin, Keith Grassel, and Jeremy Romsdahl for their dedication and assistance during the testing activities.

The authors further acknowledge Evan Ogston and Daniel Zimmerman of Schweitzer Engineering Laboratories, Inc. (SEL) for their assistance in evaluating and validating the GRE power system network.

IX. References

[1] J. Livingston, S. Marx, J. LaBlanc, Y. Gong, J. Bell, and K. Dase, "Improving Safety and Reliability on High-Voltage Lines With Broken Conductor Detection, a Utility's Perspective," proceedings of the 52nd Annual Western Protective Relay Conference, Spokane, Washington, October 2025.

[2] K. Dase, S. Harmukh, and A. Chatterjee, "Detecting and Locating Broken Conductor Faults on High-Voltage Lines to Prevent Autoreclosing Onto Permanent Faults," proceedings of the 46th Annual Western Protective Relay Conference, Spokane, Washington, October 2019.

[3] Y. Gong, G. Juvekar, and K. Dase, "Zero-Setting Broken Conductor Detection Method Using Local Measurements Only," proceedings of the 50th Annual Western Protective Relay Conference, Spokane, Washington, October 2023.

[4] W. O'Brien, E. Udren, K. Garg, D. Haes, and B. Sridharan, "Catching Falling Conductors in Midair—Detecting and Tripping Broken Distribution Circuit Conductors at Protection Speeds," proceedings of the 42nd Annual Western Protective Relay Conference, Spokane, Washington, October 2015.

[5] S. K. Lau and S. K. Ho, "Open-Circuit Fault Detection in Distribution Overhead Power Supply Network," *Journal of International Council on Electrical Engineering*, 7:1, pp. 269–275, 2017.

[6] Y. Yin, H. Bayat, N. Dunn, M. Leyba, M. Webster, A. Marquez, K. Tran, and A. Torres, "High-Speed Falling Conductor Protection for Electric Power Transmission Systems," proceedings of the 49th Annual Western Protective Relay Conference, Spokane, Washington, October 2022.

[7] K. Dase, J. Colwell, and S. Pai, "Novel Methods for Detecting Conductor Breaks in Power Lines," proceedings of the 76th Annual Conference for Protective Relay Engineers, College Station, Texas, March 2023.

[8] *SEL-411L Advanced Line Differential Protection, Automation, and Control System Instruction Manual.*

[9] Southern Electrical Equipment Company, "Phase-Over-Phase 3-Way." Available: seecoswitch.com/phase-over-phase.

[10] R. McDaniel and M. Thompson, "Impedance-Based Directional Elements—Why Have a Threshold Setting?" proceedings of the 48th Annual Western Protective Relay Conference, Spokane, Washington, October 2021.

X. Biographies

Joe Livingston received his BS in electrical engineering from North Dakota State University in 1993. After graduation, Joe worked at Minnesota Power, where he had previously interned, as a planning engineer and then as a relay engineer. He joined Great River Energy (GRE) in 1997 as a transmission planning engineer and quickly transitioned to a substation design engineer. He is presently a principal engineer responsible for protection system standards and maintenance. In this role, he primarily conducts protection system post-event analysis and ensures company compliance with various North American Electric Reliability Corporation (NERC) standards. Joe is the chairperson of the North American Transmission Forum (NATF) System Protection Practice group and an active contributor sharing knowledge of protection system operations and fault analysis. Joe is a registered professional engineer in the state of Minnesota.

Dustin Neubauer received his BS in electrical engineering from Michigan Technological University in 2006, with a focus on power systems and engineering enterprise. He began his career at Ulteig Engineers in 2007 as a substation design engineer, where he designed physical layouts and relaying/control schemes for substations. In 2009, Dustin joined Great River Energy (GRE), where he has advanced to the role of principal engineer. At GRE, he has worked extensively on the High-Voltage Direct Current (HVdc) control system, has developed and implemented the NERC CIP compliance program for the Transmission division, and performs protection system design for substations. Dustin is widely respected for his expertise in protection system operations, compliance, and fault analysis, and his collaborative approach to solving complex engineering challenges. He is a registered professional engineer in the states of Minnesota, North Dakota, and Wisconsin.

Kanchanrao Dase earned his Bachelor of Engineering degree in electrical engineering from Sardar Patel College of Engineering, University of Mumbai, India, in 2009. He completed his Master of Science degree in electrical engineering from Michigan Technological University in 2015. From 2009 to 2014, he worked as a manager at Reliance Infrastructure Limited, with a substation engineering and commissioning profile. He is currently a senior engineer in the Research and Development division at Schweitzer Engineering Laboratories, Inc. (SEL). His interests include power system protection, substation automation, and fault locating. He is a senior IEEE member and a

registered professional engineer (PE) in Washington state. He has authored several technical papers and currently holds seven patents.

Josh LaBlanc received his BS in electrical engineering from the University of North Dakota in 2011. After graduation, Josh worked for an oil and gas pipeline company, Enbridge Energy, then an electric power utility, Minnesota Power. Josh has most recently spent 6.5 years working as an application engineer for Schweitzer Engineering Laboratories, Inc. (SEL). His primary roles are providing application and technical support and training on power system protection topics. Josh is a registered professional engineer in the state of Minnesota.

Aravindkumar Rajakumar earned his Bachelor of Engineering degree in electrical and electronics engineering from Sri Sivasubramaniya Nadar College of Engineering, Anna University, India, in 2020. He completed his Master of Science degree in electrical and computer engineering from Purdue University, West Lafayette, Indiana, in 2024. Aravindkumar is currently a power engineer in the Research and Development division at Schweitzer Engineering Laboratories, Inc. (SEL). His research interests include power system protection, dynamic modeling and simulation of electric power systems, and the development of software tools for power system analysis.

© 2026 by Great River Energy and Schweitzer Engineering Laboratories, Inc.
All rights reserved.
20261021 • TP7264-01